Reusable conductimetric array of interdigitated microelectrodes for the readout of low-density microarrays

ARTICLE *in* ANALYTICA CHIMICA ACTA · JUNE 2014

Impact Factor: 4.51 · DOI: 10.1016/j.aca.2014.04.064 · Source: PubMed

7 AUTHORS, INCLUDING:

Diana Bonilla

7 PUBLICATIONS **54** CITATIONS

SEE PROFILE

J.-Pablo Salvador

Centro de Investigación Biomédica en Red e…

36 PUBLICATIONS **291** CITATIONS

SEE PROFILE

M-Pilar Marco

Spanish National Research Council

186 PUBLICATIONS **4,392** CITATIONS

SEE PROFILE

César Fernández-Sánchez

Spanish National Research Council

93 PUBLICATIONS **1,135** CITATIONS

SEE PROFILE

analytical chemistry

ARTICLE

pubs.acs.org/ac

Electrical Readout of Protein Microarrays on Regular Glass Slides

Diana Bonilla,[†] Maria Mallén,[†] Roberto de la Rica,[‡] César Fernández-Sánchez,[*,†] and Antonio Baldi[*,†]

[†]Instituto de Microelectrónica de Barcelona, IMB-CNM (CSIC), Campus UAB, 08193, Bellaterra, Spain

[‡]Supramolecular Chemistry and Technology, MESA+ Institute for Nanotechnology, University of Twente, Enschede, The Netherlands

Supporting Information

ABSTRACT: A new approach for the electrical readout of microarrays prepared on regular glass slides, using an array of impedimetric transducers (interdigitated electrodes, IDEs) is presented in this work. Impedance detection relies on the use of a urease-labeled immunoassay scheme. Urease is able to produce an increase in conductivity by hydrolysis of the urea substrate, which is measured with the IDEs and directly related to the amount of target analyte. Unlike previous electrical microarrays, the assay does not take place on top of the transducers but on a regular glass slide, which may enable the development of compact multiplexed analytical systems with lower cost per assay. A droplet of solution with the enzymatic substrate is deposited on each transducer of the array, and the microarray is positioned at a short distance (300 μm) so that each droplet wets one transducer and one spot of the microarray. This procedure allows reusing the transducer array for readout of a virtually unlimited number of microarrays. A microarray based on an immunoassay for the detection of a mouse generic protein in a concentration range from 0.03 to 30 μg mL^{-1} was carried out to assess the performance of the electrical readout approach. A sigmoid response with a limit of detection of 0.1 μg mL^{-1} and a dynamic range of 1 order of magnitude was obtained. A comparative study was also carried out with two well established analytical procedures. First, the urease-based immunoassay was tested in a 96 well microtiter plate using phenol red pH indicator and absorbance detection. Second, the microarray was carried out using the same target protein concentration range but applying a Cy3 label and fluorescence detection. Both assays allowed for the validation of the performance of the presented electrical readout system.

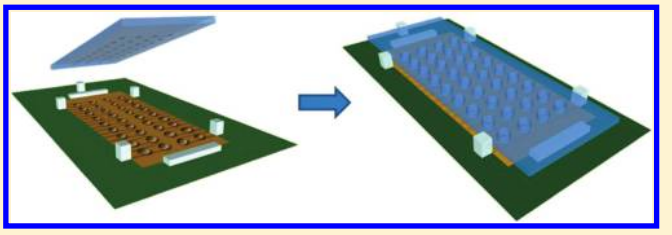

Microarray platforms with different biological components (e.g., DNA, proteins, antibodies, peptides, carbohydrates, cells, or tissue) are being developed and commercialized as powerful high-throughput analytical tools with application in genomics,[1] proteomics,[2] drug discovery,[3] or clinical diagnostics.[4] The amount of target analyte on each spot of the array is estimated by detecting a label attached to one of the molecules involved in the biorecognition event. The readout system of the microarray is, therefore, adapted to detect (and sometimes quantify) the type of label being used in the assay. The most frequently used labels generate fluorescent,[5] chemiluminiscent,[6] or colorimetric[7] signals, which are detected with optical equipment (e.g., confocal scanner). More recently, electrical readout approaches have also been proposed as an alternative that could enable more compact and inexpensive equipment. Point-of-care (PoC) diagnostics[8] or decentralized screening[9] applications could benefit from such compact readout systems. These microarray systems could also be advantageous compared to traditional analytical methods, such as enzyme linked immunosorbent assays (ELISA) on microtiter plates, by reducing assay time and volume of reagents.[10] Electrical readout microarrays consist of chips containing arrays of electrodes (two or more per spot), which translate the presence of a label related to the concentration of the target analyte into a measured impedance or current. For example, variation of conductance between electrodes has been recorded following a DNA hybridization event by means of a Au nanoparticle label and a Ag reduction reaction.[11] Another conductometric approach consists of creating Ag nanowire bridges in nanogaps between electrodes by a direct metallization of hybridized mRNA strands.[12] Biorecognition events in microarrays have also been detected through the measurement of faradaic currents recorded using electroactive labels[13] or enzymatic labels that generate electroactive products.[14−16] Redox-cycling of the enzymatic products have also been used to enhance the response.[17,18] All these electrical microarray platforms are indeed arrays of biosensors, since the biorecognition elements are attached to the transducers. The substrates of the microarrays have to be processed in clean-room facilities to form metal microelectrodes and connection tracks and pads at their surface and, subsequently, have to be encapsulated to protect electrical contacts and include connectors for the connection to the external readout instrumentation. Since microarrays are generally single use, the fabrication of these microarray substrates involves an increase in their cost and, hence, in cost per assay, that

Received: November 9, 2010
Accepted: January 11, 2011
Published: February 02, 2011

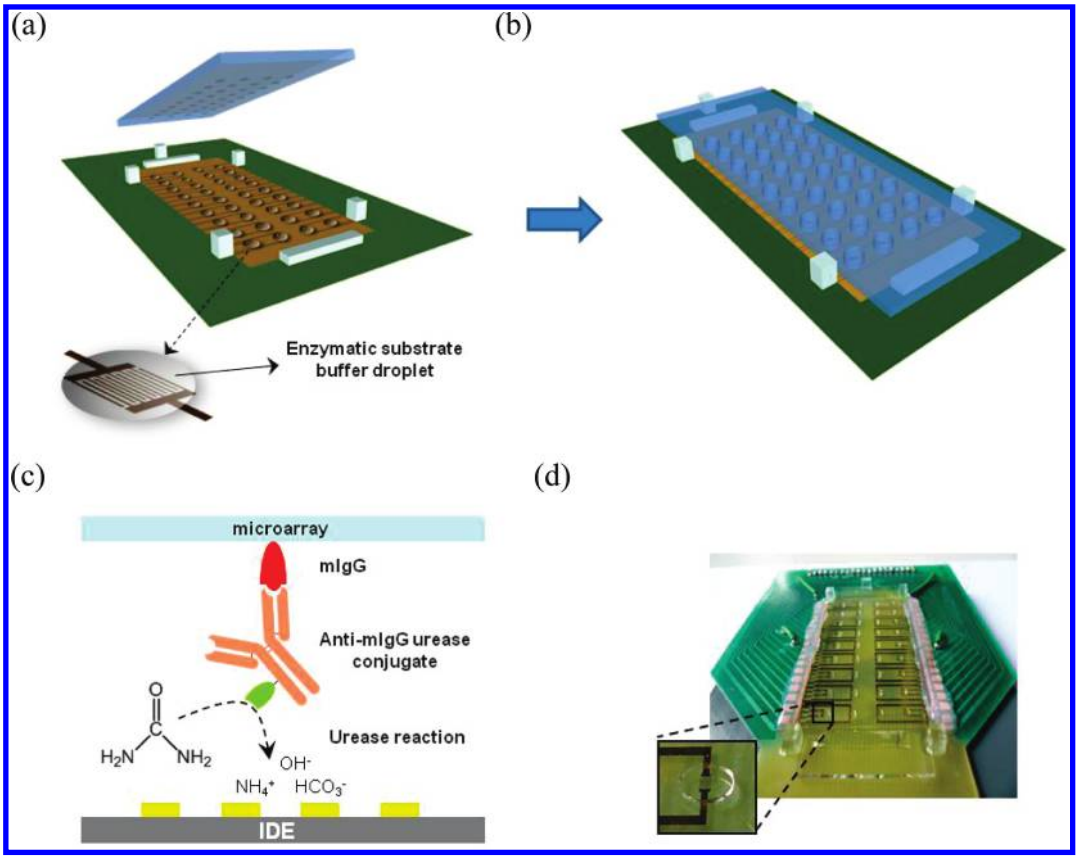

Figure 1. Overview of the electrical readout device and its working principle. 3D representation of the transducer array and protein microarray before (a) and during (b) the readout process. (c) Transduction principle: Urease labels increase conductivity by producing charged species, which is detected with IDEs transducers. (d) Photograph of the device during the readout of a glass slide protein microarray. Inset: Close view of a substrate solution droplet wetting one transducer and one spot on the microarray.

may hamper their widespread application. Here, an alternative microarray electrical readout approach is shown. The transducers were fabricated on a substrate different to the one where the assay was performed, both substrates being in close proximity in order to carry out the readout process. This configuration enables the reading of a virtually endless number of microarrays fabricated on low-cost regular glass slide substrates, in a similar fashion to optical readout systems, but with the added advantage of being more compact and cost-effective.

EXPERIMENTAL SECTION

Principle of the Electrical Readout System. The general concept of the proposed electrical readout approach is as follows: The microarray on a glass slide is aligned on top of a matching array of transducers, each transducer being covered with a droplet of solution (Figure 1a). The microarray surface is positioned at a short distance (300 μm) from the transducer array surface so that each droplet wets one transducer and one spot of the microarray (Figure 1b). The solution droplet contains enzymatic substrate that is converted into products at a rate proportional to the amount of enzyme in the spot (Figure 1c). The transducers, in turn, produce a signal proportional to the product concentration and, hence, to the enzyme label concentration. This general concept has been put into practice using urease as the enzymatic label and interdigitated electrodes (IDEs) as transducers. Urease produces an increase in conductivity of the solution by the conversion of the noncharged substrate (urea) into charged products (ammonium, bicarbonate, and hydroxide ions), while the IDEs in turn convert the increase in conductivity into an increase in conductance at a given frequency. A similar transduction approach has already been validated by our group for individual biosensors[19] with the immunoassay taking place directly on the surface of the transducer. The use of urease conjugates in immunoassays has also been previously reported. This enzyme offers several advantages over other more common labels such as peroxidase or alkaline phosphatase.[20] Urease is a stable enzyme with a higher turnover number than those enzymes mentioned above, when working under optimum conditions of pH and T. Besides, urea substrate solutions are stable for long periods of time and are innocuous to the worker and the environment.

Transducer Array Design and Fabrication. The array contains 36 (4 rows × 9 columns) gold IDEs, each IDE having 13 fingers 500 μm in length, 20 μm in width, and spaced 20 μm. This spacing ensures that the electric currents generated during the readout measurement will be confined in a thin layer of solution next to the transducer surface, so that variations in droplet shape and position have negligible effect on the measured conductance. Indeed, 80% of the current will flow in a layer not higher than 20 μm above the surface.[21] Both rows and columns of the array are spaced 6 mm apart.

The transducer array chip was fabricated at the CNM-IMB clean room according to standard photolithographic techniques. Fabrication starts with a Ti/Ni/Au trilayer sputtering deposition on 100 mm-wide, 500 μm-thick Pyrex glass wafers. Next, the

dx.doi.org/10.1021/ac102938z |*Anal. Chem.* 2011, 83, 1726–1731

Ti/Ni/Au trilayer is patterned by consecutive wet etchings in 49 wt % HF/H_2O/propylene glycol (1:10:33, v/v/v), 70 wt % HNO_3/H_2O (1:4, v/v), and 40 wt % I_2/53 wt % KI/H_2O (1:1:15, v/v/v). *Caution: HF and HNO_3 are corrosive products; safety laboratory equipment should be used during their manipulation.* Finally, a passivation coating consisting of 300 nm of silicon oxide and 700 nm of silicon nitride is deposited and patterned using plasma equipment. In this latter step, the passivation is removed from the connection pads at the edge of the chip and from the interdigitated areas. After sawing the wafer to the final chip dimensions (29 mm wide, 54 mm long), the transducer array is glued and wire-bonded to a printed circuit board (PCB). Wire bonds are subsequently protected with a silicone (3140, Dow Corning). Polymethylmetacrilate (PMMA) and glass positioning structures are also glued on the surface of the PCB to enable an easy alignment between the glass slide microarray and the readout chip. Figure 1b shows their distribution. Two 800 μm-thick glass chips are used for vertical positioning so that the surface of the glass slide is kept at 300 μm from the planar IDE transducers. Five PMMA rectangular posts are used to guarantee sufficient horizontal alignment between microarray spots and transducers. To assemble the PMMA posts in the right position, a microarray of colored solution (Congo red) was spotted on a glass slide, which after drying left red circles that enabled an easy alignment with the transducer array under the microscope. Next, the PMMA posts were glued to the PCB so that one of their sides made contact with the aligned glass slide. Figure 1d shows a picture of the encapsulated transducer array with solution droplets and a glass slide microarray in its position.

Instrumentation. IDEs transducers allow row−column interconnection and addressing, which greatly simplifies the instrumentation. The readout electronic circuit consists of four AC voltage sources (one per row) and nine current-to-voltage blocks (one per column), which are together able to measure the impedance at the terminals of the 36 IDEs (Figure S1, Supporting Information). Readout is performed row by row, that is, while one row is excited with an AC voltage source, the other rows are grounded. The input impedance of the current-to-voltage converter is virtually zero and connected to ground. Therefore, the IDEs not being excited in a column have both terminals at 0 V potential, so that the current flowing through the excited IDEs is going entirely to the current-to-voltage measurement circuit. This analysis is valid for ideal electronic components. The analysis of the real circuit and calculations of the expected cross-talk can be found in the Supporting Information. The instrumentation is partially implemented with a multifunction I/O data acquisition (DAQ) device (NI USB-6259, National Instruments) that has four analog output channels for the AC excitation of the array and sixteen analog input channels for the recording of the signals at the output of the current-to-voltage blocks. The system is controlled from a personal computer with a LabView interface, which is used to synchronize the voltage excitation and current readout while also calculating and recording the impedance for each transducer in the array at specified time intervals.

Chemicals and Materials. Urease from Jack Bean (Type C-3, ≥600 000 units/g solid), urea, phosphate buffered saline (PBS) tablets, bovine serum albumin (BSA), Tween 20, mouse immunoglobulin G (mIgG), antimouse IgG (whole molecule)-biotin antibody (anti-mIgG-biotin), and streptavidin-Cy3 were purchased from Sigma-Aldrich (Spain). The Lightning-Link Streptavidin conjugation kit (Innova Biosciences Ltd.) was purchased from Antibody BCN (Spain) and used to obtain a streptavidin−urease conjugate. Nexterion Slide AL (Schott AG) glass slides were purchased from Isogen Life Science, S.L. (Spain). All other chemicals were of analytical grade.

Development of the Urease Labeled Protein Microarray. Commercially available aldehyde-modifed glass slide substrates were used that enabled covalent anchorage of the corresponding biomolecule. mIgG was chosen as a generic target protein in order to assess the readout system performance. Following a reverse-phase-like immunoassay format[22] (Figure 1c), serial dilutions of a mIgG stock solution were prepared in PBS. The final mIgG concentration ranged between 30 ng mL^{-1} and 30 μg mL^{-1}. A 0.2 μL aliquot of each dilution was spotted in quadruplicate on the glass slide using a microdispenser instrument (iTWO model from M2-Automation, Berlin) and then incubated in a humidity chamber for 1 h at room temperature (RT). Following a washing step in PBS containing 0.1% Tween 20 (PBS-T), the slides were blocked in PBS containing 1% BSA (PBS−BSA) overnight at 4 °C. The following incubation steps of the resulting microarray were carried out using a homemade incubation chamber. It consisted of a glass substrate having the same dimensions of the glass slide to which a 0.5 mm-thick PDMS frame was bonded. First, 1 mL of a 30 μgmL^{-1} anti-mIgG-biotin solution in PBS was dispensed in this incubation chamber, and then, the microarray was placed upside down so that it got in contact with the solution and in turn sealed the chamber to avoid any solvent evaporation. After a 1 h incubation step at RT, the microarray was rinsed three times in PBS-T and further incubated in 1 mL of a 1/10 dilution of the streptavidin−urease conjugate stock solution in PBS for 1 h at RT, in the same fashion as above. The microarray was finally rinsed in PBS-T three times and then kept immersed in PBS until the readout measurement was carried out (not longer than 1 h). Before that, it was rinsed in a 250 mM glycine buffer solution and carefully dried under a nitrogen stream.

Readout Procedure. A 1.7 μL droplet of a 250 mM glycine buffer solution (pH 6.1) containing 0.1 M urea was cast onto each transducer using the microdispenser. The microarray was positioned over the transducer array so that each droplet wetted one transducer and one spot in the protein microarray. Wet pieces of tissue where distributed around the microarray to create a humid atmosphere and avoid droplet evaporation. The urease enzymatic reaction was allowed to proceed for 30 min while impedance values were registered at 10 s intervals. Before starting with the readout of a new microarray, the transducers were rinsed with deionized water to remove any residues of the enzymatic reaction products left by the previous microarray readout.

RESULTS AND DISCUSSION

Characterization of the Transducers and Readout Instrumentation. Solutions with different conductivities in the range from 10 to 120 μS/cm, prepared by diluting a concentrated KCl solution and measuring the final conductivity with a conductimeter (μCM 2202, CRISON), were used to characterize the response of the IDEs to conductivity. Droplets (1.7 μL) of solution where deposited on the transducers, and their impedance spectra were recorded with an impedance analyzer (SI 1260 SOLARTRON Impedance Analyzer; 10 kHz to 1 MHz frequency range, 0 V DC potential, and 50 mV AC peak-to-peak amplitude). The Bode plot of the impedance spectra at different conductivities (Figure 2) shows the typical shape for a pair of

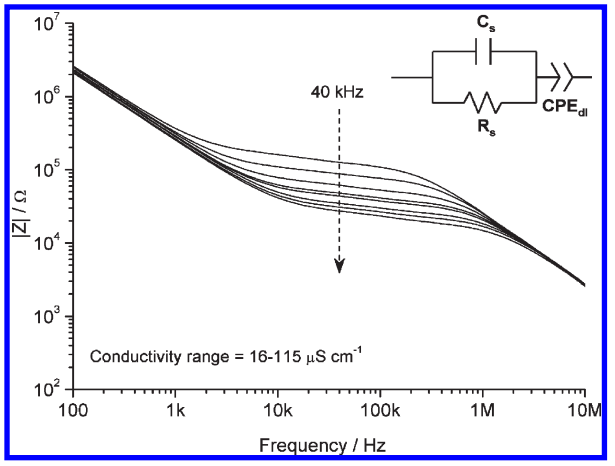

Figure 2. Bode plot of the impedance spectra of a single IDE transducer measured with an impedance analyzer while covered with droplets of KCl solutions having different conductivities (top curve 16 μS cm^{-1}, bottom curve 115 μS cm^{-1}). Inset: Equivalent circuit of the KCl solution and its interface with the metallic electrodes.

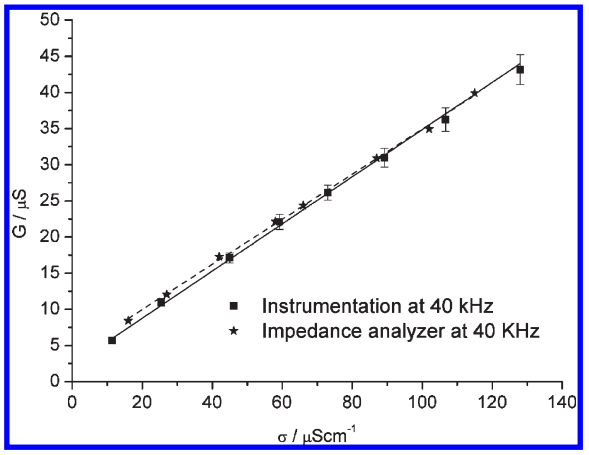

Figure 3. Average response of the 36 IDEs to conductivity of the solution when measured with the DAQ-based instrumentation. The response obtained for a single IDE with a Solartron 1290 impedance analyzer is also shown for comparison.

electrodes in solution without charge transfer processes. These spectra can be associated to the simple equivalent circuit represented in the inset of Figure 2, where the constant phase element (CPE_{dl}) corresponds to the double layer capacitance and the resistor (R_{sol}) and capacitor (C_{sol}) are related to the conductivity and permittivity of the solution, respectively. These results show that the flat portion of the curves are dominated by the conductivity of the solution and that measurement of the real part of the impedance at a single frequency in this region should give values directly proportional to the resistance of the solution between electrodes and inversely proportional to its conductance. Figure 3 shows the average conductance (G, calculated as the inverse of the real part of the impedance) of the 36 IDEs in the array for different solution conductivities (σ) measured at 40 kHz with the DAQ-based instrumentation. The relative standard deviation of G values is less than 6.3% for all the measured conductivities, which shows a good reproducibility of the fabricated transducers. The conductance values obtained with the impedance analyzer for a single IDE are also shown for comparison.

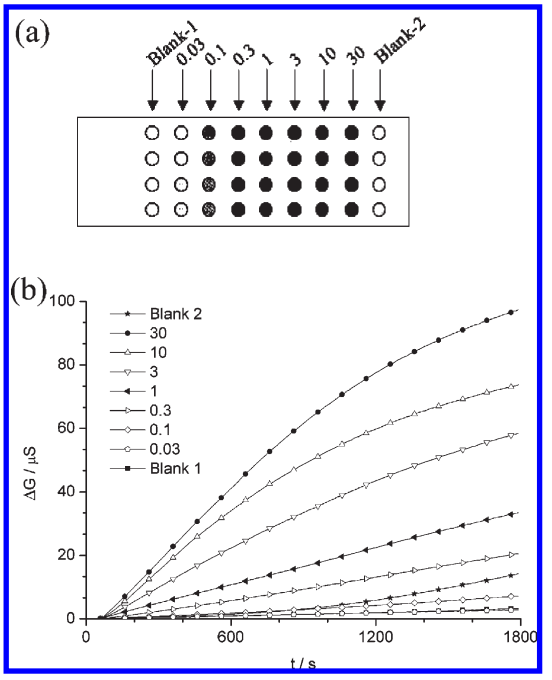

Figure 4. (a) Layout of mIgG concentrations (in μg mL^{-1}) in the test microarray. (b) Measured increase in conductance ($\Delta G \equiv G - G(t = 100\ s)$) versus time for one spot of each column in the microarray.

The response to conductivity is linear, as expected, and the values obtained with the developed DAQ-based instrumentation are in good agreement with those obtained with the impedance analyzer. The cell constant of the IDEs, defined as $k = \Delta\sigma/\Delta G$, where ΔG is the increase in conductance expected for an increase $\Delta\sigma$ in solution conductivity, is estimated as the inverse of the slope of the linear regression of the data shown in Figure 3 and yields 3.07 cm^{-1} (data from DAQ-based instrumentation). Maximum cross-talk for the range of conductance values expected in the present immunoassays produces a variation of 3.1% in the measured impedance. More details of the cross-talk measurements can be found in the Supporting Information.

Electrical Readout of the Protein Microarray. mIgG was chosen as a generic target protein to test the capability of the system to carry out the readout of microarrays with urease labels. Seven dilutions of the mIgG stock solution ranging from 0.03 to 30 μg mL^{-1} were arrayed together with a blank solution (PBS containing no mIgG). Figure 4a shows the layout of the resulting array. Two columns of blank spots were added, one next to the spots with higher concentration (Blank-1) and the other next to the spots with the lower concentration (Blank-2), so that chemical cross-talk and contamination issues could also be tested. Figure 4b shows the conductance response profiles obtained for the spots of one row. As expected, the spots with higher mIgG concentration produced a larger increase in conductance. Higher mIgG concentration results in higher concentration of urease label, which in turn results in higher enzymatic reaction rates. The concentration of urea substrate in the droplets is high enough so as to be considered constant during the readout time. Therefore, the reaction rate, and consequently the increase in product concentration with time, should also be constant. Since conductivity is proportional to concentration in dilute solutions of charged species, the rate of increase in measured conductance (i.e., the slope of the conductance vs time curve) should be proportional to the amount of label in the spot, and

dx.doi.org/10.1021/ac102938z |Anal. Chem. 2011, 83, 1726–1731

therefore, it is used as the analytical signal here. However, from this analysis, one would expect a constant rate of conductance increase, which is not the case for all the curves in Figure 4b. Following is a discussion of the second order effects leading to nonideal responses. During the first seconds of measurements, the conductance signal exhibits a small steplike response, possibly due to dissolution of traces of ionic species remaining in the array after the washing steps (Figure S2a, Supporting Information). A short delay in the order of tens of seconds from the time the urease buffer droplets contacted the microarray and the time the signal started to increase at a constant rate was also observed (Figure S2b, Supporting Information). This is likely to be related to the time it takes for the products to diffuse from the microarray substrate to the surface of the IDEs. Since these phenomena have no analytical significance, the increase in conductance was recorded after 100 s from the time the microarray was positioned on top of the IDEs array, when all the signals were already increasing at a constant rate.

Figure 4b shows two other additional phenomena: (1) The signals corresponding to the higher mIgG concentrations start to saturate after 10 min of measurement. (2) The Blank-2 signals, which are next to the spots having the higher mIgG concentration, start to increase faster than the Blank-1 signals after 15 min of measurement. The former could be attributed to a change in pH produced by the enzymatic reaction, which generates OH^- ions. Urease activity has a strong dependence in pH, showing its maximum at around pH 7.[23] However, the 250 mM glycine present in the urea substrate solution has enough buffer capacity to maintain the pH at values close to 7 during the time of measurement. This was tested by carrying out the enzymatic reaction in a larger volume of the same substrate solution and measuring the pH at the point when an equivalent change in conductivity was reached. The pH changed from an initial value of 6.15 to a final value of 7.34, which implies that the activity does not fall but slightly increases during the readout process in the spots with higher enzymatic label concentration. Another possible explanation of the saturation effect could be the evaporation of products at the boundary of the droplet. This had already been observed in urease-based ELISA assays carried out in 96 well microtiter plates.[24] The increase in conductance seen at Blank-2 spots compared to Blank-1 spots indicate that some degree of chemical cross-talk could be taking place. This could also be related to the evaporation of products at the boundary of the droplets with higher concentration, which subsequently redissolved in the neighboring droplets having less concentration, which also occurred with the urease-based ELISA assays.[24] In order to avoid the error that would cause the evaporation of enzymatic products, the slope of the conductance response between 100 and 600 s was chosen as the analytical signal, which is directly related to the enzymatic activity at the spot. The slope was calculated in this interval as the slope of the linear regression fitted with the least-squares method.

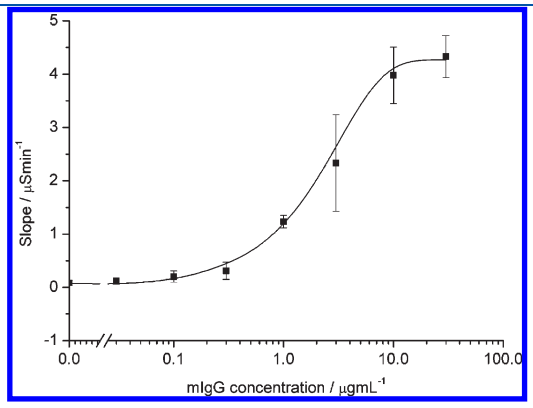

Figure 5. Results of the electrical readout showing average slopes for the signals from different mIgG concentration spots in the range of 0.03−30 μg mL^{-1}.

Figure 5 shows the semilogarithmic calibration plot obtained in the mIgG concentration range assayed. A dose−response sigmoid curve fitted to the data is also shown. This is the expected trend of most immunoassay formats. Each point is the mean value of the four replicates carried out for each analyte concentration in the microarray, the error bars corresponding to the standard deviation. The limit of detection, estimated as the minimum concentration measured with the system whose corresponding signal is equal to or higher than the mean value of the blank signal plus three times its standard deviation, is 0.1 μg mL^{-1}. The corresponding dynamic range expands roughly over 1 order of magnitude.

The performance of the urease-based immunoassay was assessed by carrying out an ELISA assay in 96 well microtiter

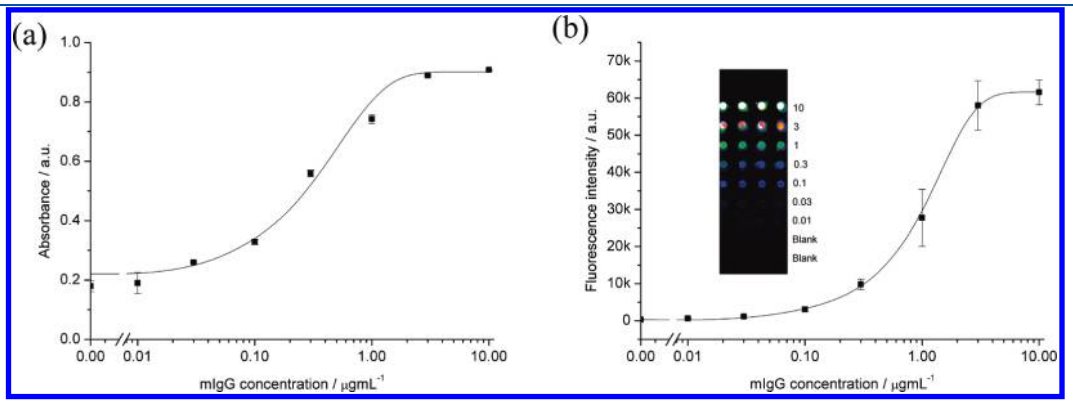

Figure 6. Results of the comparative studies. (a) Calibration plot for ELISA performed in 96 well microtiter plates using urease labeling and phenol red as a pH indicator. Each point is the absorbance mean value of the two measurements carried out for each analyte concentration, and the error bars represent the corresponding standard deviation. (b) Cy3 labeled microarray immunoassay read with a fluorescence scanner. Each point is the fluorescence intensity mean value of four measurements carried out for each analyte concentration, and the error bars represent the corresponding standard deviation. Inset shows an image of the scanned microarray (mIgG concentrations are in μg mL^{-1}).

dx.doi.org/10.1021/ac102938z |*Anal. Chem.* 2011, 83, 1726–1731

plates. Absorbance detection was possible by adding phenol red pH indicator (gradual color transition from yellow to red over the pH range 6.8−8.2) to the urea measuring solution (0.1 M urea in 250 mM glycine buffer, pH 6.1). A detailed description of the ELISA approach can be found in the Supporting Information. The corresponding calibration curve (Figure 6a) also showed the typical sigmoid behavior like the one obtained from the electrical readout of the microarray. The limit of detection, calculated as above, was 0.03 μg mL^{-1}, the dynamic range being also of 1 order of magnitude. In spite of the good performance of urease-based immunoassays, their use has been rather limited probably due to the fact that most enzymatic reactions in other reported immunoassays were carried out in solutions at pHs quite far from the optimum urease pH, which were necessary when working with pH indicators other than phenol red.[20,24] Moreover, false positives were recorded due to the migration with time of enzymatic products, especially ammonia, from one well to the adjacent ones. These drawbacks were minimized in our system using a more suitable pH and a shorter enzymatic reaction time.

Finally, in order to compare our microarray readout approach using urease conjugates with the widespread fluorescent-based microarray readout, a mIgG microarray was prepared with streptavidin−Cy3 conjugates (please, see Supporting Information for details). A similar trend of the plotted calibration curve (Figure 6b) was also observed. The dynamic range was also of 1 order of magnitude, and the estimated limit of detection using the same criterion as above was 0.01 μg mL^{-1}. This is 1 order of magnitude lower than the one achieved with our system. Nevertheless, it is anticipated that an improvement of its limit of detection will likely be achieved by optimization of the urease−streptavidin conjugation as well as by decreasing the volume of substrate solution droplets used for the readout process. Besides, it is worth noticing that a generic immunoassay was used to proof our electrical readout approach and to compare it with two well established multiplexed immunoanalytical procedures and that real limits of detection will depend on the specific application and the selected microarray assay format.

CONCLUSIONS

The electrical readout of protein microarrays on regular glass slides has been demonstrated. A readout device based on an array of interdigitated transducers and a row−column measurement instrumentation was implemented for that purpose. This device was used to read test microarrays based on the use of urease label and an immunoassay for the detection of a mouse immunoglobulin generic protein. The response was similar to the one obtained with a fluorescent scanner following the same microarray format but using a Cy3 label.

In this first prototype, the spacing of the spots was designed to be large enough to facilitate the alignment between the reader and the microarray without sophisticated mechanical clamping. Increasing spot density in future designs will imply working with smaller droplet volumes and a shorter gap between the reader and microarray substrates. In this regard, integration of fluidic systems for the rapid formation of the substrate solution droplets on each spot[16] should help with making the readout procedure more straightforward. These fluidic systems can also be used for the automation of the immunoassay steps,[25] which is necessary for the development of compact and low cost microarray analytical platforms that can be used outside the laboratories in decentralized screenings and PoC applications.

ASSOCIATED CONTENT

Supporting Information. Additional information as noted in text. This material is available free of charge via the Internet at http://pubs.acs.org.

AUTHOR INFORMATION

Corresponding Author

*E-mail: cesar.fernandez@imb-cnm.csic.es (C.F.-S.); antoni.baldi@imb-cnm.csic.es (A.B.).

REFERENCES

(1) Lockhart, D. J.; Winzeler, E. A. *Nature* **2000**, *405*, 827–836.
(2) Chen, G. Y.; Uttamchandani, M.; Lue, R. Y.; Lesaicherrea, M. L.; Yao, S. Q. *Curr. Top. Med. Chem.* **2003**, *3*, 705–724.
(3) Khnouf, R.; Olivero, D.; Jin, S.; Coleman, M. A.; Fan, Z. H. *Anal. Chem.* **2010**, *82*, 7021–7026.
(4) Hartmann, M.; Sjödahl, J.; Stjernström, M.; Redeby, J.; Joos, T.; Roeraade, J. *Anal. Bioanal. Chem.* **2009**, *393*, 591–598.
(5) Shalon, D.; Smith, S. J.; Brown, P. O. *Genome Res.* **1996**, *6*, 639–645.
(6) Zhou, D.; Qiao, W.; Yang, L.; Lu, Z. *Anal. Biochem.* **2006**, *351*, 26–35.
(7) Kristensen, R.; Gauthier, G.; Berdal, K. G.; Hamels, S.; Remacle, J.; Holst-Jensen, A. D. L. *J. Appl. Microbiol.* **2007**, *102*, 1060–1070.
(8) Arruda, D. L.; Wilson, W. C.; Nguyen, C.; Yao, Q. W.; Caiazzo, R. J.; Talpasanu, I.; Dow, D. E.; Liu, B. C-S. *Expert Rev. Mol. Diagn.* **2009**, *9*, 749–755.
(9) Lalvani, A.; Pareek, M. *Brit. Med. Bull.* **2010**, *93*, 69–84.
(10) Bellevillea, E.; Dufvaa, M.; Aamandb, J.; Bruunc, L.; Clausend, L.; Christensen, C. B. V. *J. Immunol. Methods* **2004**, *286*, 219–229.
(11) Park, S.-J.; Taton, T. A.; Mirkin, C. A. *Science* **2002**, *295*, 1503–1506.
(12) Chen, X.; Roy, S.; Peng, Y.; Gao, Z. *Anal. Chem.* **2010**, *82*, 5958–5964.
(13) Dill, K., Liu, R. H., Grodzinski, P., Eds. In *Microarrays: Preparation, Microfluidics, Detection Methods, and Biological Applications*; SpringerLink: New York, 2009, pp 247−260.
(14) Kojima, K.; Hiratsuka, A.; Suzuki, H.; Yano, K.; Ikebukuro, K.; Karube, I. *Anal. Chem.* **2003**, *75*, 1116–1122.
(15) Roth, K. M.; Peyvan, K.; Schwarzkopf, K. R.; Ghindilis, A. *Electroanalysis* **2006**, *18*, 1982–1988.
(16) Marchand, G.; Delattre, C.; Campagnolo, R.; Pouteau, P.; Ginot, F. *Anal. Chem.* **2005**, *77*, 5189–5195.
(17) Schienle, M.; Paulus, C.; Frey, A.; Hofmann, F.; Holzapfl, B.; Schindler-Bauer, P.; Thewes, R. *IEEE J. Solid-St. Circ.* **2004**, *39*, 2438–2445.
(18) Lin, Z.; Takahashi, Y.; Kitagawa, Y.; Umemura, T.; Shiku, H.; Matsue, T. *Anal. Chem.* **2008**, *80*, 6830–6833.
(19) de la Rica, R.; Baldi, A.; Fernández-Sánchez, C. *App. Phys. Lett.* **2007**, *90*, 074102.
(20) Lo, C. Y.; Notenboom, R. H.; Kajioka, R. *J. Immunol. Methods* **1988**, *114*, 127–137.
(21) Van Gerwen, P.; Laureyn, W.; Laureys, W.; Huyberechts, G.; De Beeck, M.-O.; Baert, K.; Suls, J.; Sansen, W.; Jacobs, P.; Hermans, L.; Mertens, R. *Sens. Actuators, B: Chem.* **1998**, *49*, 73–80.
(22) Pirnia, F.; Pawlak, M.; Thallinger, G. G.; Gierke, B.; Templin, M. F.; Kappeler, A.; Betticher, D. C.; Gloor, B.; Borner, M. M. *Proteomics* **2009**, *9*, 3535–3548.
(23) Blakeley, R. L.; Zerner, B. *J. Mol. Catal.* **1984**, *23*, 263–292.
(24) Echevarría, M. G.; Nosetto, E. O.; Etcheverrigaray, M. E. *J. Vet. Diagn. Invest.* **2000**, *12*, 266–268.
(25) Seidel, M.; Niessner, R. *Anal. Bioanal. Chem.* **2008**, *391*, 1521–1544.